

# Microstructure evolution and tribological properties of TiB<sub>2</sub>/Ni–Ta cermets

Luboš Bača<sup>a,\*</sup>, Zoltán Lenčoš<sup>b</sup>, Christian Jogl<sup>a</sup>, Erich Neubauer<sup>c</sup>, Martin Vitkovič<sup>b</sup>,  
Andreas Merstallinger<sup>a</sup>, Pavol Šajgalík<sup>b</sup>

<sup>a</sup> Aerospace & Advanced Composites GmbH, A-2444 Seibersdorf, Austria

<sup>b</sup> Institute of Inorganic Chemistry, Slovak Academy of Sciences, Dúbravská cesta 9, SK-845 36 Bratislava, Slovakia

<sup>c</sup> RHP-Technology GmbH & Co. KG, Forschungs- und Technologiezentrum, A-2444 Seibersdorf, Austria

Available online 15 November 2011

## Abstract

Cermets containing TiB<sub>2</sub> and single or mixed metals were produced by conventional hot-pressing technique at 2100 °C for 1 h. Nickel, tantalum and their mixtures were used as alloying substances to enhance the density of TiB<sub>2</sub> composites. The influence of metal addition on the microstructure and tribological properties were investigated. The addition of Ta powder greatly refined the microstructure of sintered samples. Similarly, the mixture of Ni and Ta metals hindered the grain growth of TiB<sub>2</sub> particles during the hot-pressing while the samples were sintered up to 98% of theoretical density. The wear behaviour of the composites was assessed by ball on disk tests. The wear rate against alumina counterbody varied in the range of  $(5.9\text{--}21.2) \times 10^{-6} \text{ mm}^3/\text{Nm}$ . The friction coefficient was not affected significantly by the alloying substances and only slightly increased from 0.58 for pure TiB<sub>2</sub> to 0.67 for samples with Ta addition.

© 2011 Elsevier Ltd. All rights reserved.

**Keywords:** Hot-pressing; Microstructure-final; Wear resistance; Borides; Wear parts

## 1. Introduction

The development of new ceramic–metal composites (cermets) is of increasing interest because they can enhance the fracture toughness of pure polycrystalline ceramics without or with minimum negative impacts on the other properties. Additionally, the presence of metals in ceramics can significantly lower the sintering temperature and increases their relative density. The densification of pure TiB<sub>2</sub> requires high sintering temperatures and long time what induce abnormal grain growth and thus lower mechanical properties of the final product.<sup>1</sup> For that reason TiB<sub>2</sub>–metal composites are studied which represent a promising class of materials for technological applications under extreme conditions due to their excellent combination of mechanical, electrical and thermal properties. In addition these composites are regarded as a good alternative for wear resistant applications, e.g. as a forming dies and cutting tools in continuous turning.<sup>2,3</sup>

Ferber et al.<sup>4</sup> observed that the addition of 1.4 wt.% Ni permits the densification of TiB<sub>2</sub> by hot-pressing at 1400 °C and the grain growth was inhibited. Moreover, the microcracking

associated with larger grains was also hindered. Nickel matrix TiB<sub>2</sub> composites were recently prepared by pulse plasma sintering combined with combustion synthesis already at temperatures from 1150 °C up to 1300 °C under load of 60 MPa.<sup>5</sup> This concept evokes to use refractory metals with higher melting points as a bonding phase for TiB<sub>2</sub> ceramics. Tantalum represents a group of metals with one of the highest melting points (3017 °C), superior chemical resistance, high hardness and preserves its ductility, even in alloys, to high temperatures.<sup>6</sup>

In order to improve the sintering performance and wear properties of TiB<sub>2</sub> ceramics, the addition of Ni–Ta metal mixtures were explored. Single metal Ni–TiB<sub>2</sub> and Ta–TiB<sub>2</sub> composites were also prepared for the comparison and better understanding of chemical processes in Ni–Ta–TiB<sub>2</sub> system.

## 2. Experimental

The powder mixtures were prepared by mixing of commercial TiB<sub>2</sub> powder (grade D, ABCR, Germany) with Ni micro-powder ( $d \leq 37 \mu\text{m}$ , Alfa Aesar) and Ta micro-powder ( $d \leq 44 \mu\text{m}$ , ABCR, Germany). The powder compositions listed in Table 1 were mixed in isopropanol with ZrO<sub>2</sub> milling balls ( $d = 3 \text{ mm}$ ) in the turbular mill for 12 h. The dried powder was screened through 125  $\mu\text{m}$  sieve. The powders were sintered by

\* Corresponding author.

conventional hot-pressing at 2100 °C for 1 h under vacuum. The phase composition was identified by powder X-ray diffraction analysis (X-pert, Philips).

Dry sliding friction and wear tests were carried out in ball-on-disk configuration without lubricant in air at room temperature. The friction tests were performed at the following set parameters: a normal load of 5 N or 10 N with alumina ball ( $d = 6$  mm), cycles of 1000 and 28,647 respectively, and a speed of 0.005 m/s. The surface morphology of discs and wear tracks were examined by scanning electron microscopy coupled with EDAX analysis (FESEM, Carl Zeiss SUPRA™ 40VP) and optical profilometry (VEECO NT1100). The abrasive area of alumina balls was investigated by optical microscopy. A common equation was used to compute the wear rate:

$$V_i = k_i F s$$

where  $V_i$  the wear volume,  $k_i$  the specific wear rate coefficient,  $F$  is the normal load, and  $s$  the sliding distance.

### 3. Results and discussion

#### 3.1. Microstructure, phase composition

The densities of TiB<sub>2</sub>-based cermets prepared by conventional hot-pressing at 2100 °C under vacuum are listed in Table 1. The density measurements revealed that the addition of pure Ni improved the density of bulk TiB<sub>2</sub> composites. On the other hand, the addition of 1 vol.% Ta only slightly improved the density of TiB<sub>2</sub>, contrary to that with 3 vol.% Ta aid. The highest densities were achieved for the mixed Ni + Ta additives and it can be concluded that with the proper ratio of Ni:Ta aids the density of pure TiB<sub>2</sub> can be significantly enhanced up to 98% of theoretical density, in comparison to the pure TiB<sub>2</sub> (85.6% T.D.).

The microstructure of TiB<sub>2</sub>-1Ni sample is shown in Fig. 1. The TiB<sub>2</sub> grains were grown abnormally up to 50–60 μm caused by nickel addition. At the higher temperatures nickel was squeezed out of hot-pressed sample due to its relatively low melting point (1453 °C). The small amount of segregated phase was found at the grain boundaries and triple junctions (Fig. 1b). The electron probe analysis (EDX) revealed some impurity spots of nanosized ZrO<sub>2</sub> (Fig. 1c) originating from the milling balls. Similar microstructure was also observed in the TiB<sub>2</sub> samples alloyed with 3 vol.% Ni.

Remarkable change in the microstructure was observed in the TiB<sub>2</sub> samples with 1 or 3 vol.% Ta aid after sintering at 2100 °C for 1 h. Tantalum addition greatly refined the microstructure of sintered sample (Fig. 2). The detailed observations revealed that the TiB<sub>2</sub> grains are surrounded by thin Ta layer, however also some Ta agglomerates in the form of islands and tracks were observed (Fig. 2b and c). White spots represent the segregated Ta (Fig. 2d). This is attributed to the difference in the particle size between Ta and TiB<sub>2</sub> starting powders ( $d_{Ta} \leq 44$  μm,  $d_{TiB_2} = 3.5$ –6.0 μm), in spite of 12 h homogenization with 3 mm zirconia balls in TURBULA® Shaker-Mixer. Moreover, tantalum is rather stable in TiB<sub>2</sub> matrix, because according to the thermodynamic data available in the literature the Gibbs free energy of formation for TiB<sub>2</sub> is –347.87 kJ/mol

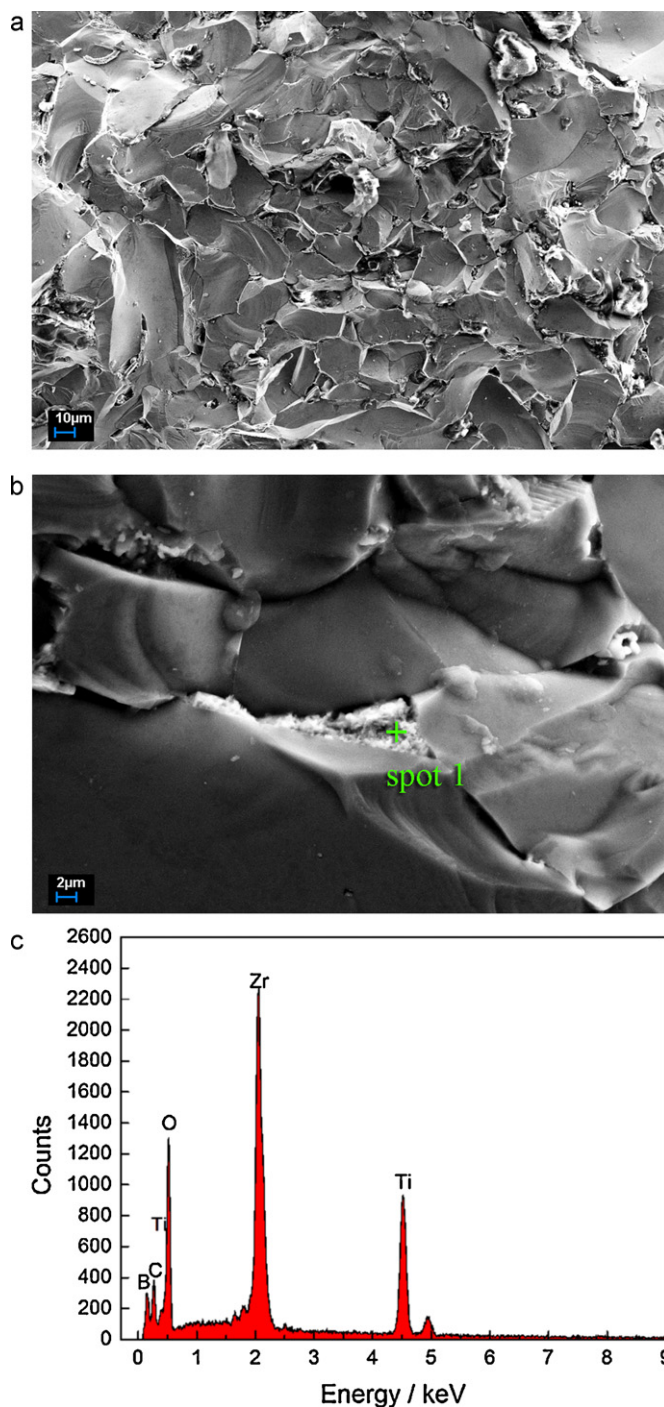


Fig. 1. (a) Microstructure of TiB<sub>2</sub>-1Ni composite sintered at 2100 °C for 1 h; (b) segregation of nanosized ZrO<sub>2</sub> in triple junctions and (c) EDX analysis of such impurities.

and for TaB<sub>2</sub> it is –191.02 kJ/mol at 2000 K.<sup>7</sup> Thus the formation of TaB<sub>2</sub> by reaction of Ta with TiB<sub>2</sub> is less preferable and the added Ta powder can hinder the grain growth of TiB<sub>2</sub> during sintering by segregation on the grain boundaries. However, Kokabi et al. observed that TaB<sub>2</sub> in the contact with TiB<sub>2</sub> forms the Ti(Ta)B<sub>2</sub> solid solution, which induces lattice strain and limited grain growth.<sup>8</sup>

Further change in the microstructure of TiB<sub>2</sub> cermets was observed, when the combination of alloying elements

Table 1

Metal content and densities of TiB<sub>2</sub>-based cermets prepared by hot-pressing at 2100 °C for 1 h.

Sample	Metal content (vol.%)	Measured density (g cm <sup>-3</sup> )	Theoretical density (g cm <sup>-3</sup> )	Density (%)
TiB <sub>2</sub> –1Ni	1Ni	4.39	4.54	96.7
TiB <sub>2</sub> –3Ni	3Ni	4.40	4.62	95.2
TiB <sub>2</sub> –1Ta	1Ta	4.14	4.63	89.3
TiB <sub>2</sub> –3Ta	3Ta	4.67	4.86	96.1
TiB <sub>2</sub> –1.5Ni + 1.5Ta	1.5Ni + 1.5Ta	4.64	4.75	97.6
TiB <sub>2</sub> –0.5Ni + 2.5Ta	0.5Ni + 2.5Ta	4.74	4.83	98.1
TiB <sub>2</sub>	–	3.85	4.50	85.6

1.5Ni + 1.5Ta and 0.5Ni + 2.5Ta were used. Fig. 3a shows the back scattered SEM image of the fracture surface of TiB<sub>2</sub> cermet alloyed with 0.5Ni + 2.5Ta. Two different phases are discernible: the TiB<sub>2</sub> matrix phase is surrounded with very well distributed second phase. Due to the Ni addition to Ta the homogeneity of alloying phase remarkably increased, compared to the samples with only Ta addition. The lowest eutectic temperature in the binary Ni–Ta system is 1366 °C<sup>9</sup> and thus Ni helps to redistribute also Ta metal at the used sintering temperature. Moreover, tantalum can diffuse into the TiB<sub>2</sub> structure at higher temperatures and form the Ti<sub>1-x</sub>Ta<sub>x</sub>B<sub>2</sub> solid solution.<sup>8</sup>

Except Ni and Ta also Ti is present in the studied system, although in the form of TiB<sub>2</sub>. It is known that titanium in its β b.c.c. structure forms a continuous solid solution with tantalum.<sup>10</sup> Ansel et al. calculated the interdiffusion coefficient in Ta–Ti system over the whole range of compositions.<sup>11</sup> They found that the interdiffusion coefficient behave anomalously and nonlinearly decreases with the tantalum concentration at high temperatures. In agreement with the results from the literature mentioned above it is most probable that due to the delayed

diffusion of Ta in TiB<sub>2</sub> at high Ta concentration, only solid solution is formed as a thin film on the surface of TiB<sub>2</sub> grains. The formation of core-rim structure was observed in TiB<sub>2</sub> cermets alloyed with 0.5Ni + 2.5Ta (Fig. 3a and b). The EDX line analysis across the grain boundary revealed a drop of Ti content close to the grain boundary and the increase of Ta signal intensity. It can be concluded that the limited tantalum diffusion and relatively short time during the sintering of TiB<sub>2</sub>–Ta based cermets favours the formation of core-rim structure. Such observations were proved by X-ray analysis of three different samples with 3Ni, 3Ta and 0.5Ni + 2.5Ta additives and are shown in Fig. 4. The XRD analysis revealed mainly TiB<sub>2</sub> and as a minor phase carbon. The presence of Ti<sub>1-x</sub>Ta<sub>x</sub>B<sub>2</sub> solid solution was also recorded and characterized by the small peak near by the main TiB<sub>2</sub> peak at 2θ ~ 51.86° (enlarged diffraction in Fig. 4).

### 3.2. Tribological properties

The influence of metal powders addition (max. 3 vol.%) on the evolution of the coefficient of friction (COF) against alumina

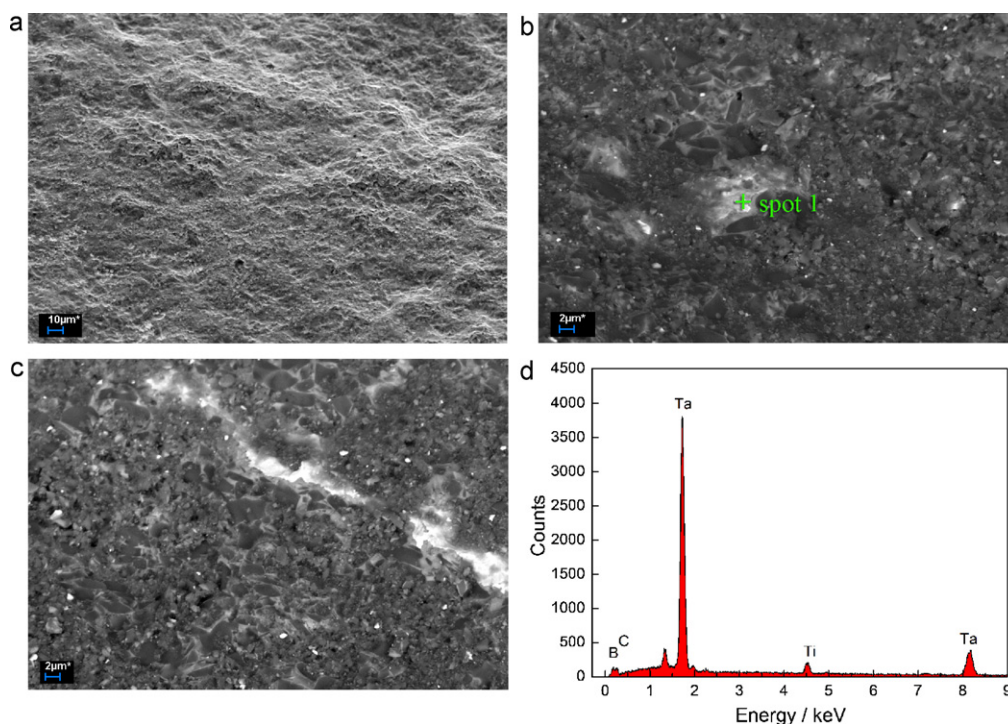


Fig. 2. (a) Microstructure of TiB<sub>2</sub>–3Ta composite sintered at 2100 °C for 1 h; (b and c) agglomerates of Ta metal in the form of islands and tracks; and (d) segregation of Ta – white spots.



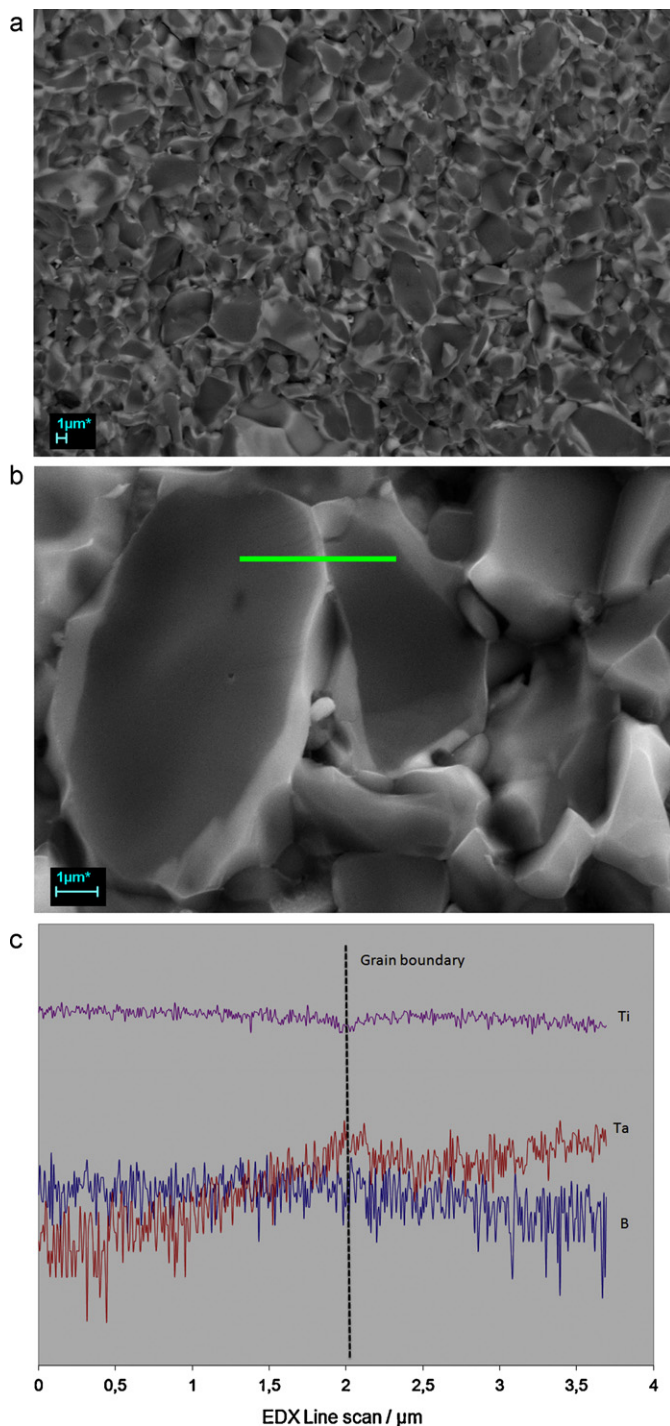


Fig. 3. Back scattered SEM image of the fracture surface of  $\text{TiB}_2$  cermet; (a) alloyed with 0.5Ni + 2.5Ta; (b and c) EDX line analysis across the grain boundary in 0.5Ni + 2.5Ta  $\text{TiB}_2$  cermet.

ball with the load of 5 N and 1000 cycles is shown in Fig. 5. All tests done during this first phase of tribological investigations were performed under identical conditions. A comparison of steady-state COF values revealed that the friction coefficient varied in the range of 0.54–0.67. The lowest COF was observed for the samples alloyed with 1 and 3 vol.% of Ni, however the wear rate was rather high compared to other samples and reached the values of  $1.27 \times 10^{-5} \text{ mm}^3/\text{Nm}$  and  $1.62 \times 10^{-5} \text{ mm}^3/\text{Nm}$ ,

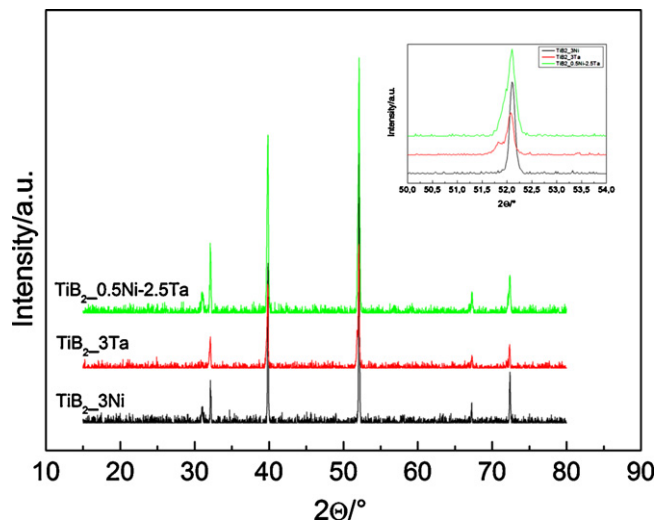


Fig. 4. XRD analysis of the  $\text{TiB}_2$  cermets alloyed with various metals. The presence of  $\text{Ti}_{1-x}\text{Ta}_x\text{B}_2$  solid solution at  $2\theta \sim 51.86^\circ$  is shown in detail.

respectively. A significant drop of wear rate was observed for the sample with 3 vol.% Ta and for the samples with combined Ni–Ta additives. The wear rate corresponds with the measured COF in these composites. It should be pointed out that also the pure  $\text{TiB}_2$  sample has slow wear rate and low/acceptable COF.

For such applications, where higher contact loads and hence substrate deformations are encountered, e.g. cutting tools, the tribological investigation at higher applied loads are necessary. To see the effect of increased applied load (10 N) on the COF and wear rate of produced cermets, the best four samples were tested from the previous set. The results are summarised in Fig. 6 and the measured values show that the friction coefficient varied in the narrower range, from 0.47 to 0.55. The comparison of the COF measured at 5 N and 10 N shows a slight decrease at higher load, especially for samples  $\text{TiB}_2$ -3Ta and  $\text{TiB}_2$ -0.5Ni + 2.5Ta. The COF of sample with 3 vol.% Ni addition remained nearly the same also under 10 N load, whereas the wear rate remarkably decreased at higher load. The drop of wear rate value at 10 N applied load was also observed

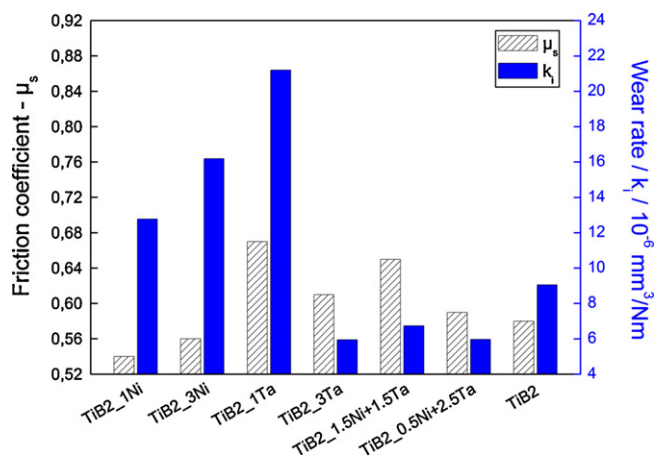


Fig. 5. Steady state values of the coefficient of friction and corresponding wear rates of Me- $\text{TiB}_2$  composites at the load of 5 N.

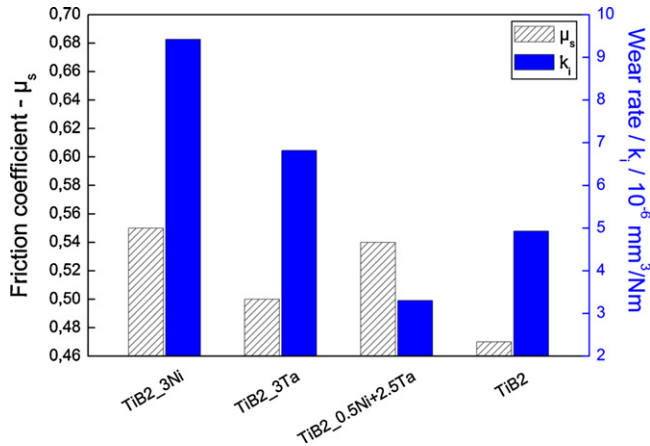


Fig. 6. Steady state values of the coefficient of friction and corresponding wear rates of selected Me–TiB<sub>2</sub> samples compared with the pure TiB<sub>2</sub> at the load of 10 N.

for the TiB<sub>2</sub>–0.5Ni + 2.5Ta sample ( $k_i = 3.3 \times 10^{-6} \text{ mm}^3/\text{Nm}$ ). On the other hand, the wear rate of samples alloyed with 3 vol. % Ta slightly increased at 10 N. Most probably in the samples with higher tantalum content at higher loads more lubricating oxides are formed via tribochemical oxidation which contribute to lower friction coefficient (e.g. the COF for Ta<sub>2</sub>O<sub>5</sub> is 0.07<sup>12</sup>). However, the overall COF of composites is limited by the friction coefficient of Ti, Ta, Ni and Al oxides or suboxides.

Surprisingly, also the not fully dense pure TiB<sub>2</sub> sample had relatively low values of COF and wear rate in comparison to the alloyed samples. The reason for such behaviour is further discussed with respect to the microstructure (Fig. 7).

Based on the previous results we decided to repeat the friction test at 5 N of applied load for the best samples, i.e. that with TiB<sub>2</sub>–0.5Ni + 2.5Ta composition, but the test was prolonged from 1000 to 28,647 cycles. The COF measurement and the calculated wear rate revealed the increase of these parameters for TiB<sub>2</sub>–0.5Ni + 2.5Ta sample to 0.65 and  $17.7 \times 10^{-6} \text{ mm}^3/\text{Nm}$ , respectively. In both tests the COF increases during the running-in phase (200 cycles) up to 0.63 and 0.68 respectively, then a little bit decreases and remains constant during the further cycles. These values of COF are typical for TiB<sub>2</sub> ceramics against another ceramic counterparts including Al<sub>2</sub>O<sub>3</sub>, mullite or SiC.<sup>13</sup>

To understand the processes running during the wear, the surface of tested samples was analyzed by SEM coupled with EDX analysis. Scanning electron micrograph (Fig. 7a) shows the wear track of TiB<sub>2</sub> disk after sliding against the alumina ball with the load of 5 N after 1000 cycles. It can be seen that the pure TiB<sub>2</sub> contains a lot of pores which serve as a reservoirs for accumulation of wear debris due to the fatigue (Fig. 7b). EDX analysis of such already filled reservoirs revealed massive oxidation of TiB<sub>2</sub> substrate due to the tribo-reaction with alumina ball (Fig. 7c) followed by the formation of thin oxide film

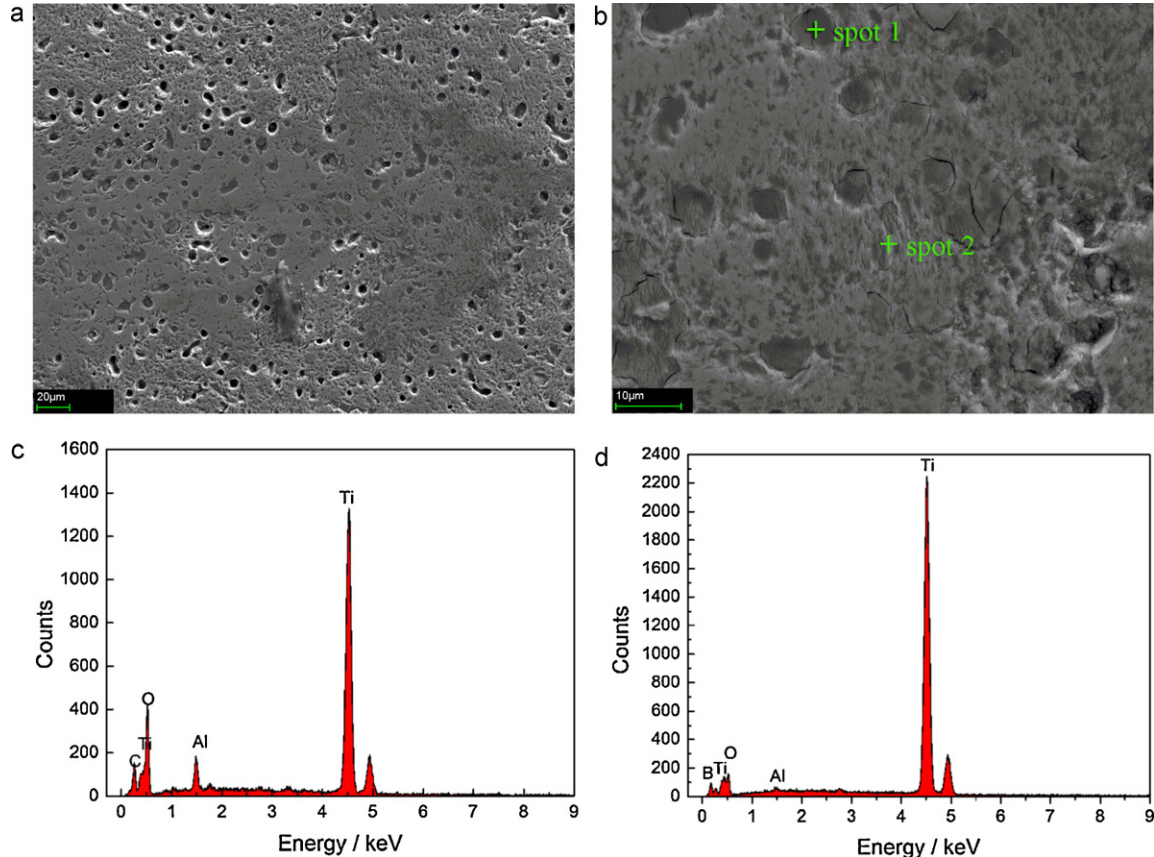


Fig. 7. SEM micrographs of TiB<sub>2</sub> sample after sliding against the alumina ball with the load of 5 N after 1000 cycles; (a) wear track; (b) pores filled with the wear debris; EDX analysis of (c) accumulated debris in pores; (d) wrinkled tribofilms.



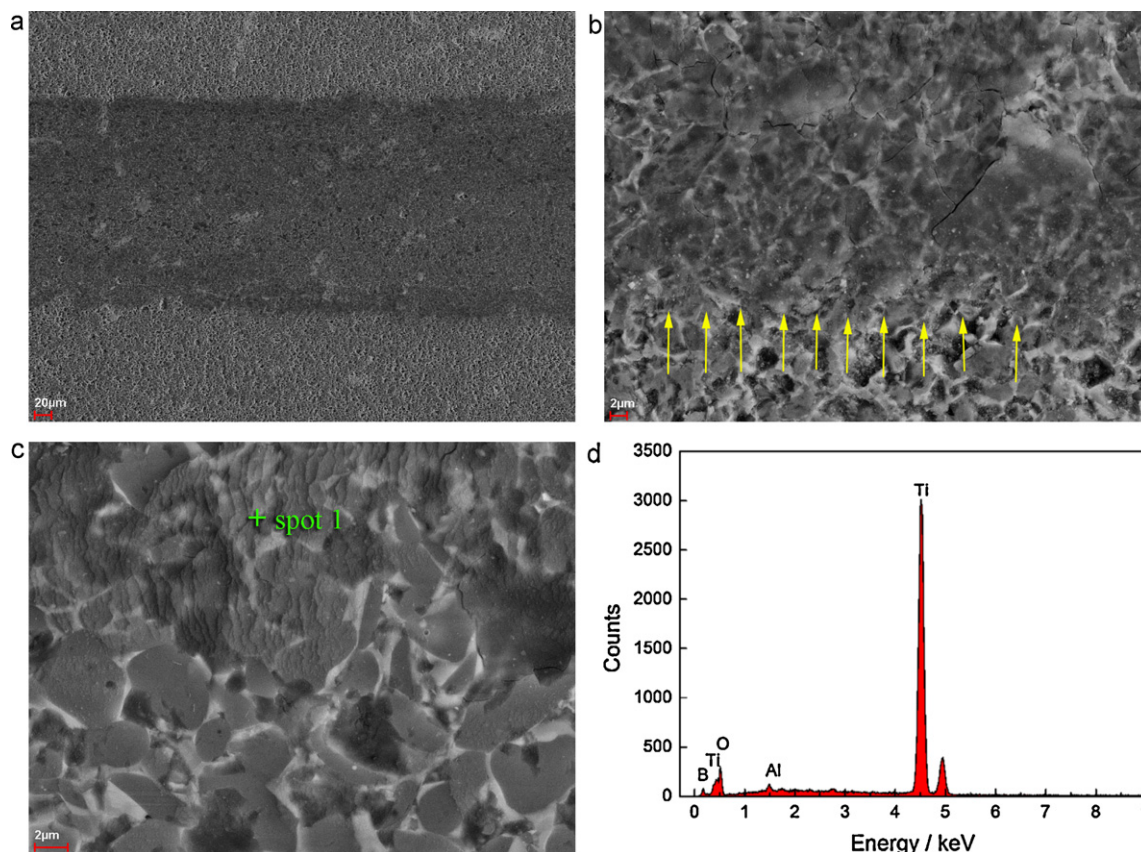


Fig. 8. SEM micrographs of  $\text{TiB}_2\text{--}0.5\text{Ni} + 2.5\text{Ta}$  sample after sliding against the alumina ball with the load of 5 N after 1000 cycles (a) wear track; (b) oxide wear debris along the edge of the track (arrows indicate the edge of the wear track); (c) thin non-continuous wrinkled film with numerous tribo-islands; (d) EDX analysis of wrinkled tribofilm.

(Fig. 7d). These results show that the tribo-oxidation is the main wear mechanism for the pure  $\text{TiB}_2$  sample.

On the other hand, the  $\text{TiB}_2$  sample alloyed with  $0.5\text{Ni} + 2.5\text{Ta}$  was sintered almost to full density with the minimum of pores. Post-test microscopic characterization of the wear track, contrary to pure  $\text{TiB}_2$ , revealed the accumulation of oxide wear debris at the head and foot as well as along the edges of track (Fig. 8a). The detailed view revealed some micro-cracks in the thick adherent tribolayer (Fig. 8b) on the border of track, and the presence of thinner non-continuous wrinkled film with numerous tribo-islands spread within the track (Fig. 8c). The EDX analysis (Fig. 8d) showed that the thin wrinkled layer contains mainly Ti, Al, and O.

When the number of sliding cycles increased to 28,647, the morphology of the analyzed worn surfaces of  $\text{TiB}_2\text{--}0.5\text{Ni} + 2.5\text{Ta}$  sample indicates that the number of sliding cycles has no influence on the wear mechanism, but only on the greater material displacement.

Fig. 9a illustrates the morphology of worn surface and the accumulation of wear scars at the “head” and “foot” of track. Due to the longer sliding distance the accumulation of scars in this sample is much higher in comparison with previous one and show higher degree of oxidation. It seems that several wear processes are present during the friction. At the beginning, during the running in phase, thin discontinuous layer is formed. With increasing time the film becomes thicker and is plastically

deformed generating wrinkled oxide morphology due to the sliding movement (Fig. 9b). When the thickness of the layer achieves the critical value and internal stresses are enough high, the films start to crack. These cracks are formed perpendicular to the sliding motion and along the folds (Fig. 8c). As the test continues, oxide debris are slowly removed from their original place and transferred to the periphery of the wear track. The EDX analysis of inner parts of tracks in various samples was carried out and proved that all debris contain mainly Ti, Al, Ta and O.

There are several mechanisms described in the literature for the material removal during the friction test of  $\text{TiB}_2$  composites. Ajayi et al.,<sup>14</sup> observed for the  $\text{SiC}\text{--}\text{TiB}_2$  ceramic matrix composite that the material removal involved failure of the particle-matrix interface, resulting in particle pull-out and chipping of the matrix material. Wäsche et al.<sup>15</sup> and Ribeiro et al.<sup>16</sup> observed the formation of wear oxide films and wrinkled morphology of the tribofilm during friction tests. The former authors observed the formation of oxide films and filling of cavities with oxide wear debris in sliding of  $\text{Al}_2\text{O}_3$  and  $\text{SiC}$  pins on the  $\text{TiB}_2$  disc.<sup>15</sup> They suggested that these cavities are formed by grain pull out during the running in wear process and act as a wear debris reservoir for the thin oxide film formed on the neighbored grains in sliding contact. On the other hand, Ribeiro et al. observed only cracking of wrinkled boronized tantalum surface due to the fatigue and perpendicular to the sliding direction.

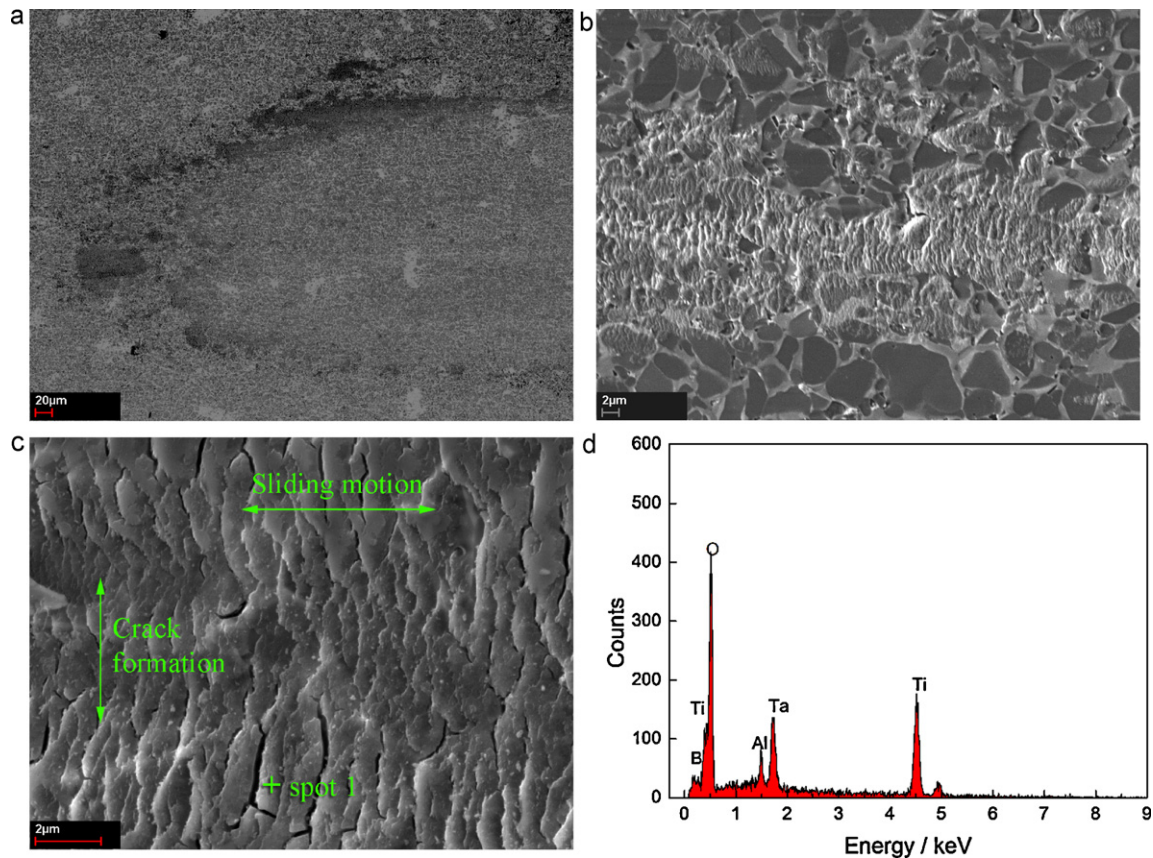


Fig. 9. SEM micrographs of  $\text{TiB}_2\text{--}0.5\text{Ni} + 2.5\text{Ta}$  sample after sliding against the alumina ball with the load of 5 N after 28,647 cycles (a) wear track; (b) oxide wear debris along inside the track; (c) cracking in wrinkled film; (d) EDX analysis of wrinkled tribofilm.

Our results also indicate that several mechanisms are present during the wear test, however the fatigue and tribochemical oxidation are identical for both the pure  $\text{TiB}_2$  ceramics as well as for the alloyed  $\text{TiB}_2$  composites, similar to the results observed by other authors.<sup>17,18</sup>

#### 4. Conclusions

Pure and metal(Ni, Ta)-bonded  $\text{TiB}_2$  ceramics were prepared by hot pressing. The results showed that with the proper ratio of Ni:Ta addition the density of  $\text{TiB}_2$  ceramics can be significantly enhanced (up to 98.1% T.D.) in comparison to the pure  $\text{TiB}_2$  (85.6% T.D.).

The microstructure observations revealed that the limited tantalum diffusion during the sintering of  $\text{TiB}_2\text{--Ta}$  based cermets favours the formation of core-rim structure. Nickel addition supports the homogeneous distribution of tantalum and its better bonding to the  $\text{TiB}_2$  grains. The formation of  $\text{Ti}_{1-x}\text{Ta}_x\text{B}_2$  solid solution was observed by the weak diffraction peak nearby the main  $\text{TiB}_2$  peak at  $2\theta \sim 51.86^\circ$  in  $\text{TiB}_2$  samples alloyed with Ni–Ta mixture.

Finally it can be concluded that the  $\text{TiB}_2\text{--}0.5\text{Ni} + 2.5\text{Ta}$  sample shows the best wear properties among all the prepared composites. The highest obtained density and the core-rim structure is most probably responsible for the better wear resistance of these samples in comparison to the other samples including

the pure  $\text{TiB}_2$ , although the COF was not improved. The binder phase (Ta) in  $\text{TiB}_2$  cermets participates in the tribochemical reactions; however nickel was not detected in the reaction products by EDX analysis. All the tribological investigations showed that the tribochemical oxidation is the predominant wear mechanism.

#### Acknowledgement

The work was supported by the FFG Research Studio under contract 818649 and Slovak grant agency VEGA 2/0178/10 and 2/0036/10.

#### References

- Wang W, Fu Z, Wang H, Yuan R. Influence of hot pressing sintering temperature and time on microstructure and mechanical properties of  $\text{TiB}_2$  ceramics. *J Eur Ceram Soc* 2002;**22**(7):1045–9.
- Horlock AJ, McCartney DG, Shipway PH, Wood JV. Thermally sprayed Ni(Cr)– $\text{TiB}_2$  coatings using powder produced by self-propagating high temperature synthesis: microstructure and abrasive wear behaviour. *Mater Sci Eng A* 2002;**336**(1–2):88–98.
- Sigl LS, Schwetz KA, Dworak U. Continuous turning with  $\text{TiB}_2$  cermets: preliminary cutting tests. *Int J Refract Met Hard Mater* 1993–1994;**12**(2):95–9.
- Ferber MK, Becher PF, Finch CB. Effect of microstructure on the properties of  $\text{TiB}_2$  ceramics. *J Am Ceram Soc* 1983;**1**:C2–3.
- Jaroszewicz J, Michalski A. Preparation of a  $\text{TiB}_2$  composite with a nickel matrix by pulse plasma sintering with combustion synthesis. *J Eur Ceram Soc* 2006;**26**:2427–30.

6. Lide DR. *Handbook of chemistry and physics*. 81st ed. Boca Raton: CRC Press LLC; 2000.
7. Bansal NP. *Handbook of ceramic composites*. New York: Kluwer Academic Publisher; 2005.
8. Kokabi VC, Shobu K, Watanabe T. Studies of the Mechanical Properties of  $\text{TiB}_2$ –6% $\text{TaB}_2$ –1% $\text{CoB}$ – $x\%$  $\text{mZrO}_2$ . *J Eur Ceram Soc* 1997;**17**: 885–90.
9. Okamoto H. Ni–Ta (nickel–tantalum). *J Phase Equilib* 2000;**21**: 497.
10. Murray JL. The Ta–Ti (tantalum–titanium) system. *Bull Alloy Phase Diagrams* 1981;**2**(1):62.
11. Ansel D, Thibon I, Boliveau M, Debuigne J. Interdiffusion in the body cubic centered  $\beta$ -phase of Ta–Ti alloys. *Acta Mater* 1998;**46**: 423–30.
12. Suzuki S. Adhesion and abrasion of sputter-deposited ceramic thin films on glass. In: Mittal KL, editor. *Adhesion measurement of films and coatings*, vol. 2. VSP BV; 2001. p. 235–46.
13. Yang Q, Senda T, Kotani N, Hirose A. Sliding wear behaviour and tribofilm formation of ceramics at high temperatures. *Surf Coat Technol* 2004;**184**:270–7.
14. Ajayi OO, Erdemir A, Lee RH, Nichols FA. Sliding wear of silicon carbide–titanium boride ceramic matrix composites. *J Am Ceram Soc* 1993;**76**:511–7.
15. Wäsche R, Klaffke D, Troczynski T. Tribological performance of SiC and  $\text{TiB}_2$  against SiC and  $\text{Al}_2\text{O}_3$  at low sliding speeds. *Wear* 2004;**256**:695–704.
16. Ribeiro R, Ingole S, Usta M, Bindal C, Ucisik AH, Liang H. Tribological investigation of tantalum boride coating under dry and simulated body fluid conditions. *Wear* 2007;**262**:1380–6.
17. Vleugels J, Basu B, Hari Kumar KC, Vitchev RG, Van der Biest O. Unlubricated fretting wear of  $\text{TiB}_2$ -containing composites against bearing steel. *Metall Mater Trans A* 2002;**33A**:3847–59.
18. Darabara M, Bourithis L, Diplas S, Papadimitiou GD. A  $\text{TiB}_2$  metal matrix composite coating enriched with nitrogen: microstructure and wear properties. *Appl Surf Sci* 2008;**254**:4144–9.